REEF3D Wave Generation Interface for Commercial Computational Fluid Dynamics Codes

Csaba Pakozdi *[1], Hans Bihs[2], and Arun Kamath[2]

[1]SINTEF Ocean, Trondheim, Norway
[2]Department of Civil and Environmental Engineering, Norwegian University of Science and Technology (NTNU), 7491 Trondheim, Norway

Journal of Offshore Mechanics and Arctic Engineering, 2021, **143** (3), pp. 031902.
DOI: http://dx.doi.org/10.1115/1.4048925

Abstract

In recent years CFD developments have shown a trend to combine RANS CFD simulation with other methods such as wave theories or velocity potential based numerical wave tanks, in order to reduce to computation costs. This is however not a new approach, and there exists a large amount of literature about domain decomposition techniques describing a two way coupling between the RANS CFD models and other methods. One can also observe an increasing popularity in the use of a less sophisticated technique where different fluid solvers are combined with one-way coupling. In these methods a predefined solution is provided in the far-field (ignoring the structure), while a three-dimensional (3D) CFD simulation is applied in a limited zone near the structure. The predefined solution is used to specify the background far-field solution. The governing equations are extended by he addition of a source term. The published solutions use wave theory or a numerical wave tank where the predefined solution is calculated parallel to the RANS solver. In this way it is possible to reduce the interpolation inaccuracy and the amount of transferred data to the CFD simulation. The disadvantage of this technique is that the far field solver has to be prepared in order to run in parallel with the CFD solver. Due to the one way coupling it is possible to predefine this information in tables before the CFD simulation. This technique makes it possible to define a general interface between difference solvers without modifying existing codes. This paper presents such a technique where the predefined solution is stored into files. An interpolation function delivers all data to the far-field solution for the CFD simulation. The paper analyses the necessary accuracy of the interpolation and the costs of the input/output operation of the CFD simulation through several verification cases.

*Corresponding author, csaba.pakozdi@sintef.no

Keywords: REEF3D; coupling; interface; RANS; coupled simulation

Postprint, published in Journal of Offshore Mechanics and Arctic Engineering,
doi:http://dx.doi.org/10.1115/1.4048925

1 Introduction

When one way coupling between different methods is established using the direct forcing method, the definition of the velocity field and the location of the fluid interface needs to be given inside the numerical domain, in the so called wave generation and relaxation zones (Jacobsen et al. (2012) and Jacobsen (2017)) in addition to the inlet and outlet boundary conditions such as in Duz et al. (2016) and Clauss et al. (2006).

If an analytical solution such as Fenton's Stokes 5^{th} order wave theory Fenton (1985) is coupled to a CFD simulation with a two-phase method (Volume of Fluid method) in Star-CCM+ Pakozdi et al. (2015), a function is used to directly calculate the velocity at the requested location and time without any interpolation in time or space. The definition of the filling degree of the cells, the volume fraction parameter, is more complicated because it must be numerically estimated from the current location of the free surface. This procedure is critical because it has a large influence on the quality of the simulation.

When a fluid solver, such as a two-phase Reynolds-Averaged Navier-Stokes Equations (RANSE) solver or a one-phase potential based numerical wave tank (PNWT), makes the calculation parallel with the coupled RANSE simulation, the definition of the velocity vector components is accomplished using lookup tables and by spatial interpolation. The volume fraction parameter (VOF) is defined in the same way as before based on the current location of the free surface elevation. This one way coupling is based on the use of predefined information as the fluid solver calculates the fluid parameters before the coupling and it is not influenced by the results from the coupled fluid solver. The two simulations run simultaneously and are synchronized in time, therefore time interpolation is not necessary. Several papers demonstrate the efficiency and correctness of such coupling, Kim et al. (2012), Bøckmann et al. (2014) and Baquet et al. (2017).

As mentioned in the abstract, one way coupling makes it possible to define this information and store it into files before starting the coupled simulation. Therefore, it is not necessary to modify the code which is coupled to the CFD solver. This technically simplifies the establishment of such as coupling. In this case the two simulations are not synchronized in time and an additional interpolation must be accomplished. The coupling technique with predefined files may introduce inaccuracies due to the additional interpolation and may increase the simulation time because of the amount of transferred data into the CFD simulation.

The objective of this paper is to show the possibility of such as coupling technique. We use linear and bi-linear interpolation to reduce the computational cost and to ensure numerical robustness. This is a lower order interpolation compared to the cubic spline interpolation which is used successfully in Jacobsen (2017) and Choi et al. (2018). We chose to implement and test this technique using REEF3D which is a two-phase RANSE solver Kamath et al. (2015) to predefine the fluid components. This code has been validated for wide range of free surface fluid phenomena such as breaking wave kinematics Alagan Chella et al. (2015),

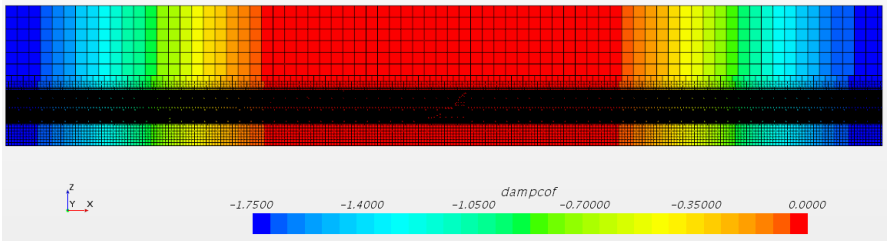

(a) Distribution of the forcing coefficient μ in the x-direction with the grid, simulation of a Stokes 5^{th} order regular wave

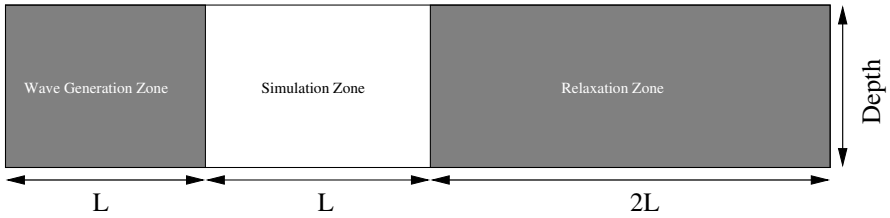

(b) Scheme of the CFD domain

Figure 1: Side view of the solution domain

steep wave kinematics Aggarwal et al. (2018), Aggarwal et al. (2017) and is used as a CFD numerical wave tank Miquel et al. (2018).

These components are transferred into the two-phase Star-CCM+ simulation Simcenter. The idea behind this decision is that a successful coupling is most likely between two two-phase RANSE solvers. Because the coupling works satisfactory with REEF3D, we also tested the method with one-phase data and the results are presented in this paper.

In this paper we present the implementation of the coupling and the verification of the coupling between REEF3D and Star-CCM+ for regular deep water waves, for regular shallow water waves and for focused waves. We generated the coupling files Fenton's Stokes 5^{th} order wave theory based on Fenton (1985), and by second order Cnoidal wave theory using in-house script functions. An in-house PNWT simulation of a focused wave group was also coupled to the CFD simulation. All of these simulations are 2D simulations which are coupled together. The verification is based on the comparison of the free surface elevation and the velocity time series just below the free surface. This technique is now also tested for a coupling between a 2D REEF3D regular deep water wave simulation with a 3D CFD simulation with a mono-pile. The same case without coupling is described in Pakozdi et al. (2018). During the 3D simulation we identified an effective way to run the simulation on the cluster to avoid additional computer costs from reading large amounts of files. The resulting force time series is compared with earlier CFD simulations presented in Pakozdi et al. (2018) with the same wave parameters.

2 Implementation

2.1 One way coupling using forcing zone

In this study we used the commercial CFD-software STAR-CCM+ from Siemens, extended by user-programming to enforce coupling with the background far-field solution, using the same but modified simulation file without structure and changed domain size. A short description of the forcing coupling taken from Pakozdi et al. (2015).

The simulation is initialized using a predefined solution. The pressure, velocities and water volume fraction are computed from the predefined data and specified as an initial solution in the solution domain. At all future time steps, predefined data is used to specify the background far-field solution in the wave generation zone and the calm water hydrostatic solution is used in the relaxation zone. The governing equations are extended by adding a source term

$$q_\phi = -\mu\rho(\phi - \phi^*) \ , \tag{1}$$

where ρ is the local fluid density (depending on local value of the volume fraction of liquid), ϕ is the solution of the equation being solved (momentum equations or volume fraction equation), ϕ^* is the background solution, and μ is the forcing coefficient. The source term in the equation for volume fraction of water does not contain density.

The forcing coefficient μ varies smoothly within the wave generation zone along the vertical boundaries at the inlet and outlet in 2D simulations, see Figure 1a. In this study, we use the $\cos^2$-variation, following recommendations by Kim et al. (2014):

$$\mu = -\mu_0 \cos^2(\pi x^*/2) \ , \tag{2}$$

where x^* is the local coordinate normal to the boundary and pointing inwards, with value 0 at the inlet boundary and 1.0 at the end of the forcing zone. Thus, the forcing coefficient (and the source term) is zero outside the forcing zone, where the original governing equations are solved. μ_0 is the maximum value of the forcing coefficient which is obtained at the boundary of the solution domain. The $\cos^2$-function is smooth and asymptotic at both ends of the range.

2.2 Data structure

The applied data structure is a modified version of the REEF3D file structure, which is used to store the status of the simulation at each time step. The data are stored in a binary file format, which reduces the file size and the file reading time. This file structure is defined only for 2D wave (long crested wave) simulations. The necessary information for coupling are the two components of the velocity field u, w and the value of the level-set function Φ at the cells. The data structure uses a structured interpolation grid with equidistant spacing in the x-direction but not in the z-direction where the spacing $dz(x_i)$ and the vertical coordinates of the lower vertical boundary line $z(x_i)_0$ is stored for each horizontal location x_i. Using a structured grid has the advantage that the coordinates of the grid points do not need to be stored explicitly. This reduces the amount of data and the identification of the active part of the interpolation grid to a given coordinate does not require the use of complex and numerically expensive algorithms.

The first part of the file contains scalar parameters such as the simulation time, the boundary box of the numerical domain, the number of cells in horizontal and vertical directions and the horizontal spacing dx. The large continues data fields contain the vector of $dz(x_i)$, the lower vertical boundary coordinates of the grid $z(x_i)_0$ and the velocity components u, w and the level-set values Φ. These are stored at the end of the files as double precision binary data. Scripts are used to generate these files from the REEF3D simulation files.

The generated interpolation files are stored in the ./dat folder in the same location as the CFD simulation file. During the 3D simulation, when the simulation is started on 2 nodes with 24 cores per node on a Linux cluster, the simulation is seen to crush. Using the absolute path to the ./dat folder the simulation starts successfully. However, a significant increase in the calculation time is observed with this solution. In order to avoid all files being read through the network, the ./dat folder is copied parallel to each involved cluster node before the simulation using the parallel shell tool `pdsh`. The copy command `cp` with the `pdsh` is called during submitting the job inside a `PBS` script. After the simulation all copied folders are removed from the nodes following this script. In this way the simulation time not increases significantly compared to the simulation running on one cluster node.

2.3 Interface to Star-CCM+

Star-CCM+ gives the user the possibility to link a user code to a simulation via a so called user code library Simcenter. The simulation can transfer the current simulation time t and the location (x, y, z) of interest into the user code through an interface function. The user code can return the required fluid properties (u, v, w and the VOF parameter) through the same interface function. Because this interface function is software specific we do not further describe the declaration of our C++ interface function called by the CFD solver.

The developed C++ interface function `table2D` does not only serve as a communication interface, but it is also the main function for the interpolation. Two C++ classes, `HeaderInfo` and `WaveTable2D`, and several utilitiies C++ functions are developed to deal with the data files management, to read the files and to interpolate in time and space. The code design is focused on finding an efficient way to minimize the memory usage and the number of file operations to avoid a significant slow down of the CFD simulation. The authors see this as a key factor for a practical implementation of the technique.

The `table2D` function accomplishes the following tasks with the use of the above mentioned functions and classes:

- creating the necessary C++ objects (HeaderInfo and WaveTable2D objects), which also includes the allocation of the necessary memory at the beginning of the simulation
- freeing all dynamically allocated memory at the end of the simulation
- completing the list of all accessible data files in the ./dat folder at the start
- setting up the time range of the interpolation files
- identifying the necessary data files for the time interpolation during the simulation
- defining the time when the next time instant interpolation file is needed to read

2.4 Syntax of the time interpolation

The interpolation functions are implemented in the WaveTable2D class as methods. All necessary information for the creation of a WaveTable2D object is defined in the first part, in the header of the data files. The C++ class, HeaderInfo, is developed to read only this part of the files. The gathered information is accessible as public properties of this class. The table2D function accomplishes the interpolation in time involving three WaveTable2D objects. Two of these objects are created during the reading of the first two data files at the start of the simulation. A bisectional search algorithm based on Press et al. (2007) locate method is used at the beginning of the simulation to identify these two data files which fit the actual simulation time. The necessary memory of these data is allocated only at the beginning of the simulation because the new data sets are always loaded into the same allocated memory of one of the two WaveTable2D objects. For the identification of the next file during the simulation, an incremental searching algorithm is implemented based on the Numerical Recipes hunt method in order to reduce the searching time. Due to these two searching algorithms the interface function can handle sets of interpolation files with adaptive time steps as well.

The HeaderInfo object is used to read the time instant of the data file and check the consistency of the data files regarding the interpolation grid size without reading the entire file. The new information containing the velocity components and the level-set values are always loaded into the object with the lowest (older) time value t_1. A swap between the pointers of these two objects takes care of the correct time sequence of these objects, i.e, $t_2 \geq t_1$ is always true.

For example, the value of u for time instant t is defined by the linear interpolation method as:

$$u(t) = u(t_1) + d\tau \left(u(t_2) - u(t_1)\right) \quad \text{with} \quad d\tau = \frac{t - t_1}{t_2 - t_1} \quad . \tag{3}$$

Because the interpolation grid does not change in time, the same $d\tau$ can be used for all variables to calculate their interpolated values only based on the time values as can be seen in (3). The velocity and level-set data field of the third WaveTable2D object are actualized at each new simulation time with its update method where (3) is used to define its actualized data sets based on the already prepared data sets of the other two WaveTable2D objects.

2.5 Syntax of the spatial interpolation

The requested velocity components (u, w) at the x, z locations are defined by the bi-linear interpolation. The bi-linear interpolation itself is applied on a parametric domain (ξ_i, τ_j) interpolation grid, which is calculated from the segment lengths of the geometrical grid:

$$\xi_i = \frac{x_i - x_0}{x_{N_x-1} - x_0} = \frac{idx}{N_x dx} = \frac{i}{N_x}, \quad i = 0, \ldots N_x - 1 \tag{4}$$

$$\tau_{i,j} = \frac{z_{i,j} - z_{i,0}}{z_{N_z-1,i} - z_{i,0}} = \frac{jdz_i}{N_z dz_i} = \frac{j}{N_z}, \quad j = 0, \ldots N_z - 1 \tag{5}$$

where N_x is the number of the cells in the horizontal direction of the interpolation grid and N_Z is the number of the cells in the vertical direction. This transformation enables the bi-linear method to interpolate on non-orthogonal interpolation grids as well. The value of $u(x, z)$ for

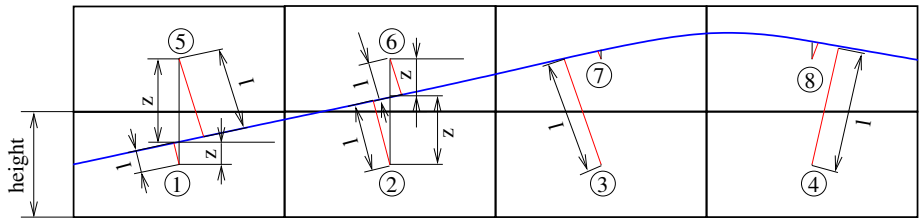

Figure 2: Estimation of the filling's degree of cells based on the level-set value

example, is estimated by using the bi-linear interpolation as:

$$u(x,z) = (1-d\tau)\,(1-d\xi)\,u_{i,j} + d\tau\,(1-d\xi)\,u_{i+1,j} + (1-d\tau)\,d\xi u_{i,j+1} + d\tau d\xi u_{i+1,j+1}. \tag{6}$$

The values of i and j are defined from the coordinates of x and z:

$$i = \text{round}\left(\frac{x-x_0}{dx}\right) \quad \text{and} \quad j = \text{round}\left(\frac{z-z(x)_0}{dz(x)}\right) \tag{7}$$

with the assumption of an equidistant distribution in the x-direction and straight vertical grids. The values of $dz(x)$ and $z(x)_0$ are defined by linear interpolation using (3) with $dz(x_i)$ or $z(x_i)$ as the interpolation data set with dx. The same values of $d\xi$ and $d\tau$ are used with the same i and j when $w(x,z)$ and $\Phi(x,z)$ are estimated. They are defined as:

$$d\xi = \frac{\frac{x-x_0}{N_x dx} - \xi_i}{\xi_{i+1} - \xi_i} \quad \text{and} \quad d\tau = \frac{\frac{z-z(x)_0}{N_z dz(x)} - \tau_j}{\tau_{j+1} - \tau_j}. \tag{8}$$

2.6 Definition of the two phase fluid

When using the two phase VOF model in the coupled CFD simulation to represent the fluid with a free surface, the location of the two fluid phases (water and air) is given by the degree of filling of each cell by the VOF parameter.

If the upper and lower limits of the free surface motion are known, i.e. the maximum wave crest height and the minimum wave trough depth, the definition of the VOF parameter is straightforward. Below the lower limit it is always equals to one, while above the upper limit it is always zero. These limits can be estimated because the two simulations do not run in parallel. For the sake of simplicity the same limits for the crest and trough heights are assumed. These upper and lower limits are then defined by a single scalar double precision variable in the interface function from Star-CCM+. This parameter must be specified by the user in the setup of the simulation.

The correctness of the VOF parameter has large influence on the shape of the generated waves in the free surface zone. If the filling degree is calculated based on the area under the free surface line shown in Figure 2, the areas under blue line yield a one cell thick interface layer. However, the shape of the reconstructed free surface line from the VOF parameter (the isoline with the value of 0.5 of the VOF parameters) may tend to have a shape similar to a

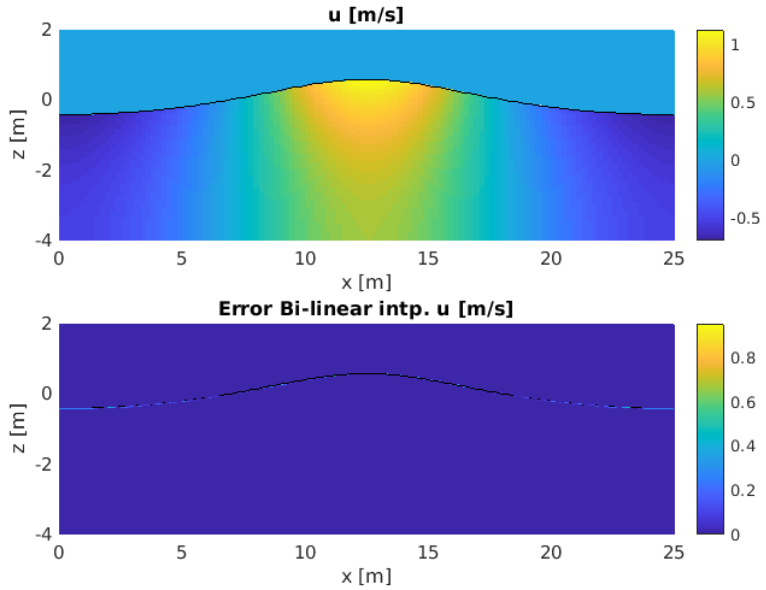

Figure 3: Interpolation error without correction of the velocity components above the free surface

step function. Therefore, we use the level-set function with the smoothed Heaviside function to define the filling degree in the free surface zone following Bihs et al. (2016):

$$VOF = \frac{1}{2}\left(1 + \frac{\Phi}{\epsilon} + \frac{1}{\pi}\sin\left(\frac{\pi\Phi}{\epsilon}\right)\right) \tag{9}$$

The level-set value Φ defines the signed distance between the cell's centroid and the location of the free surface as illustrated by the red lines in Figure 2. The level-set value is defined from the bi-linear interpolation of the REEF3D estimated level-set value Φ according to (6) at the CFD solver cell's centroid location (x, y, z). The parameter ϵ defines the thickness of the interface layer between water and air, where the VOF value changes from one to zero. The best shape is observed if the value of ϵ equals 1.6 times the cell height. The definition of this parameter is difficult because the user code only has information about the location of the cell's centroid but not the size of the cell. To overcome this issue one additional parameter is passed from the CFD simulation to the user code, the cell edge height (Figure 2) in the free surface zone. This parameter is usually constant in the area where the free surface changes its location and it must be consistent with the real mesh size in the wave generation zone. It is a user defined parameter and must be defined in the setup of the CFD simulation. The advantages of using this method are that the same procedure works with 3D data sets and that the method has no limitations regarding the free surface steepness or breaking waves. The disadvantage of the method is the interface layer thickness is larger than one cell height.

2.7 Coupling with one phase simulations

We use the same method to estimate the VOF parameter when we couple the one phase results to the CFD code. The level-set function could be calculated from the known location

of the free surface for the interpolation grid. However, if the steepness of the free surface is not extremely large, the error of using the vertical signed distance between the free surface location and the cell's centroid (defined as z in Figure **??**fig:vofestimation), instead of the real level-set value, is small ($l \approx z$). The coupled simulations based on the one phase results presented in this paper use the signed vertical distance in the interpolation files as Φ.

The accuracy of the bi-linear interpolation can significantly drop in the grids closest to the free surface by 100 % if the velocity is defined as zero in the air as shown in Figure 3. The velocity components and the level-set value Φ are calculated at the interpolation grid using Fenton Stokes 5^{th} order wave theory as shown in the left hand side of the figure. After the generation of this data set, a new data set of the fluid parameters is generated at different locations. This data set is compared with the results of the bi-linear interpolation at the new locations and the error is shown in the right hand side of the figure.

This error can be reduced if the velocity in the air directly above the free surface is defined as:

$$y_{\text{Air}} = y_\eta + (z_{\text{Air}} - \eta) \left.\frac{dy}{dz}\right|_\eta \tag{10}$$

where y_η is either the horizontal or vertical velocity component at the free surface, dy/dz is the gradient of the horizontal or vertical velocity component at the free surface and η is the vertical location of the free surface. This very simple procedure can reduce the error to an acceptable level as shown in Figure 4.

3 Verification

All ten simulations are summarized in Table 1. The different simulations are compared with each other based on the free surface elevation at the location of interest and the time series

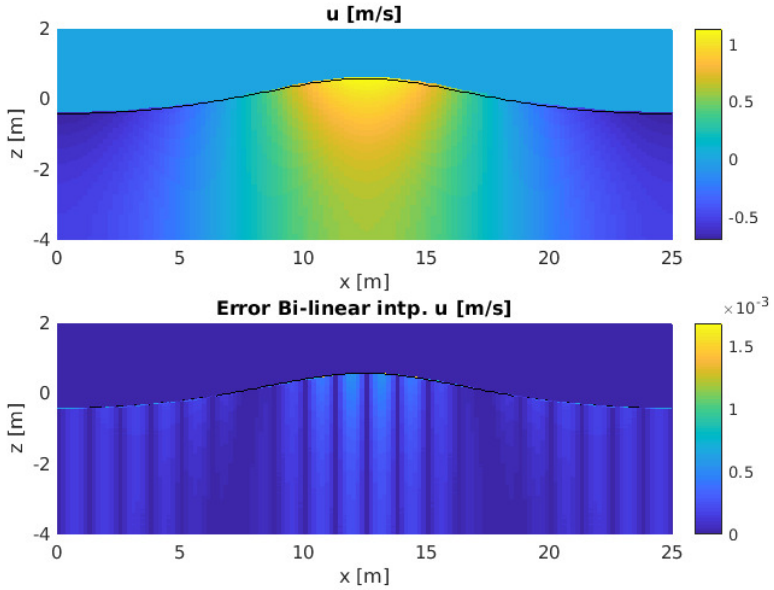

Figure 4: Interpolation error with correction of the velocity components above the free surface

Nr.	Type of wave	H [m]	T [s]	L [m]	Depth [m]	coupled with	phase	Comment
1	Stokes 5^{th} order	1.00	4.50	25.14	4.01	Star-CCM+ function	one	regular wave
2						REEF3D	two	
3						In-house script	one	
4	Cnoidal 5^{th} order	0.75	12.00	76.24	4.01	REEF3D	two	regular wave $\mu = 1.0$
5							two	regular wave $\mu = 10.0$
6	Cnoidal 2^{nd} order					In-house script	one	regular wave $\mu = 10.0$
7	Focused wave	focus point $x = 15.00$ m			4.01	REEF3D	two	
8	Focused wave	focus point $x = 126.21$ m				PNWT	one	
9	Stokes 5^{th} order	0.285	2.18	7.65	0.75	REEF3D	two	2D regular wave
10								3D with mono-pile

Table 1: Overview of all simulations

of the velocity components at one vertical location below the free surface zone.

3.1 Star-CCM+ setup

As mentioned earlier, a modified simulation file in the Pakozdi et al. (2015) is used. The two-dimensional simulations are one cell thick in the y-direction and without any structure. The length of the wave generation zone is about one wavelength and the numerical beach length is two wavelengths. The length of the domain without any influence is about a wave length (Figure 1a and 1b).

The boundary condition at the downstream side is defined by the calm water condition using Star-CCM+'s in-built function `FlatVofWave` Simcenter. In this way it is not necessary to define the velocity and the VOF parameters in the downstream relaxation zone. The initial condition is defined using the data taken from the first interpolation file in the wave generation zone and with the calm water condition in the rest of the domain. At all future time steps, the interpolation tables are used with the user code table2D to specify the background far-field solution in the wave generation zone.

The Peric's recommendation Peric (2017) is followed by creating the grid with aspect ratio 2 (dx/dz) within the free surface zone and setting the number of cells per wave height to be between 20 and 30 cells. The angle factor in the HRIC-scheme Muzaferija and Peric (1999) is set to 0.15 and the Interface Momentum Dissipation is activated in the Phase Interaction modeling (artificial viscosity is set to 0.1). The time step is constant in the Star-CCM+ simulation, 2nd-order time discretization is used and the value is set to yield a Courant number lower than 0.1 in the free surface zone. All approximations used are of the second order (midpoint rule approximation for integrals, linear interpolation and central differences). A segregated iterative procedure is used, in which the three momentum equations, the pressure-correction equation and the equation for volume fraction of water are solved in turn; the process is repeated five times within each time step in order to update non-linear terms

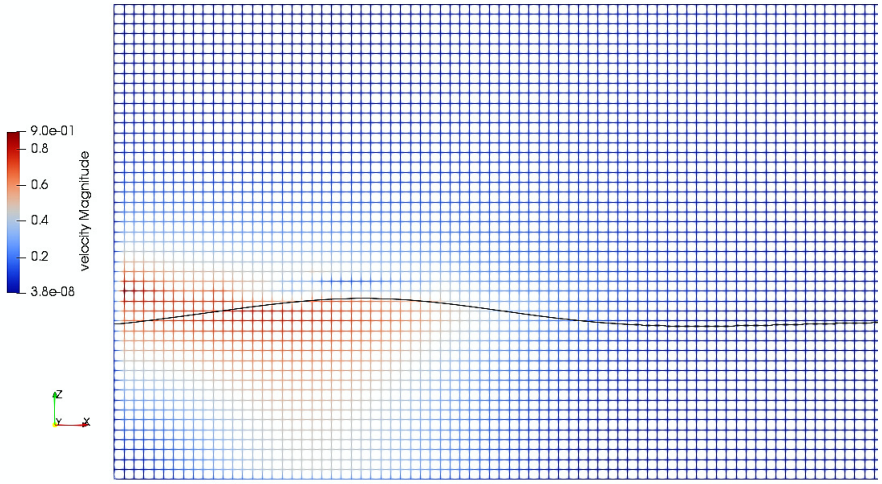

Figure 5: Mesh used in the REEF3D simulation and as interpolation grid

and account for inter-equation coupling. Under-relaxation is used to control the update of variables which is required due to non-linearity of equations. The under-relaxation factors used in this study are 0.2 for the pressure and 0.9 for the velocities and the volume fraction of water.

During the verification numerical instability was observed in the Star-CCM+ simulations at the interface between water and air as small wiggles on the free surface. There are small disturbances in the presented time series, which are caused by these wiggles. We could reproduce these effects without the coupling using only the inlet boundary condition to generate the waves. Applying a numerical damping of the waves by using stretched mesh Ostman et al. (2014) gives the same results. Therefore, we excluded the forcing zone approach as a reason for the numerical instability.

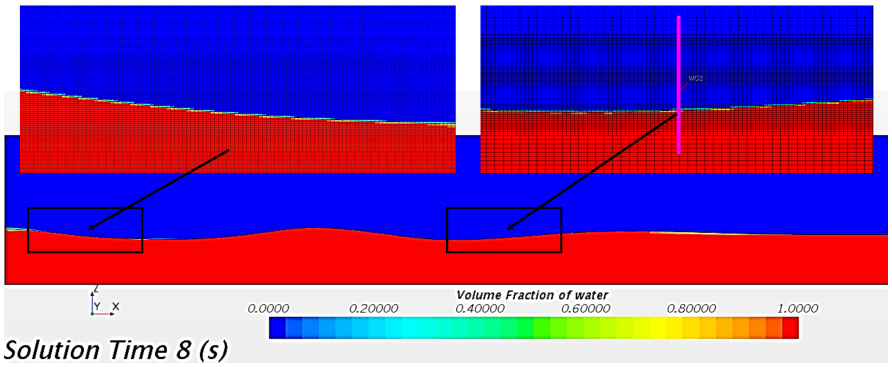

Figure 6: Volume of fraction of water in the Star-CCM+ simulation based coupled with the REEF3D simulation

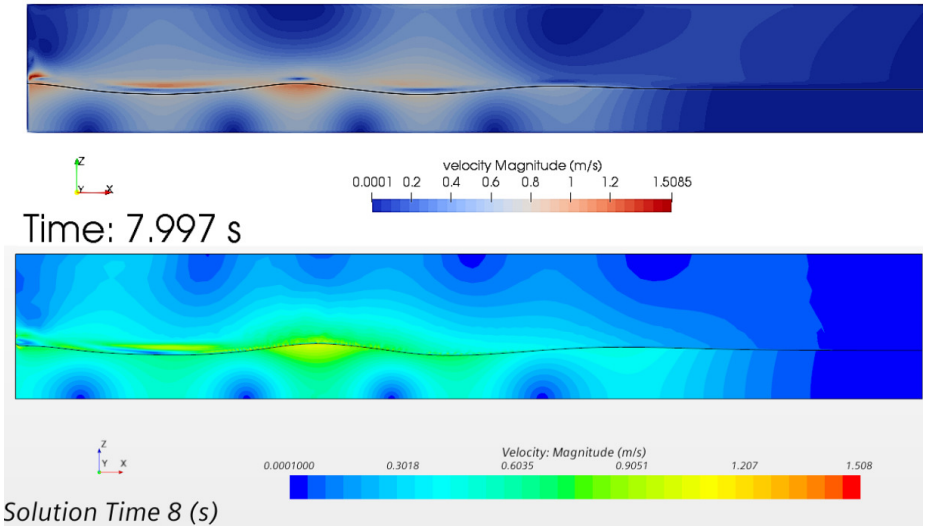

Figure 7: Comparison of the magnitude of the velocity between REEF3D simulation and Star-CCM+

3.2 Stokes 5^{th} order waves

In order to estimate how much the user code reduced the efficiency of the Star-CCM+ simulation an in-built function was used in one simulation (simulation nr. 1 in Table 1) to generate the waves. This is the `FifthOrderVofWave` function Simcenter, based on Fenton's Stokes 5^{th} order wave theory Fenton (1985). When the REEF3D simulation is coupled to the CFD simulation (simulation nr. 2) every time step from the REEF3D simulation is used directly in the interpolation files with the original REEF3D grid. REEF3D uses adaptive time steps which is limited by a given Courant number, in this simulation set to 0.1. The applied grid is uniform as shown in Figure 5 and the number of grid cells per wavelength is set to 120 in the REEF3D simulations. The accuracy of the interpolation grid is tested for the one phase simulation coupled with the CFD solver (simulation nr. 3) as described and shown in the previous paragraph and in Figure 4. The number of cells per wave length is 120 and 40 cells per wave height. A convergence study shows linear proportionality between the vertical grid resolution and the maximum interpolation error, reducing the number of cells per wave height from 40 to 20 doubles the interpolation error of the horizontal velocity component from $1.5 \cdot 10^{-3}$ to $3.0 \cdot 10^{-3}$ (not shown in this paper). The same tendency can be observed for the vertical velocity component.

The volume fraction of water is presented at the early stage of the simulation in Figure 6. The figure shows the whole domain and two close zooms of the free surface with the applied mesh. One can see the smooth interface between water and air in the wave generation zone (upper left picture) and in the simulation zone (upper right picture). The interface is about 2 cells thick in the wave generation zone and one cell thick in the simulation zone. The magnitude of the velocity field, presented in Figure 7 shows good agreement between the REEF3D simulation and the coupled CFD simulation.

A comparison of the three different simulations with the analytical solution generated by an in-house script is presented in Figure 8 to 10. The time series are synchronized with

each other at the first zero-up-crossing of the free surface time series at $t = 8$ s. After the initial transient phase, (from $t = 10$ s) one can observe good agreement between the original REEF3D results, the target time series (red line) and the CFD simulations which are coupled with REEF3D (blue line). The analytical solution (black line) shows a larger deviation from the REEF3D solution than from the Star-CCM+ in-built wave results (cyan line). This observation supports the result which was published in Pakozdi et al. (2018) and the difference in the dispersion characteristics is not discussed in this paper. The top figures demonstrate that the waves generated in Star-CCM+ using the current coupling method are the same as the waves generated in REEF3D (red and blue lines). Furthermore, one can see a very good agreement between the analytical solution, (which is now the target result, black line) and the CFD simulation based on the interpolation table generated from these results (magenta line). The same synchronization delay is used when the velocity component time series are compared in Figure 9 and 10. The same behavior as in the comparison of the free surface curves can be seen. This comparison verifies that the implemented one way coupling between the difference results and the CFD solver works.

All simulations were executed on one node with 3 cores, the number of cells is about 73000 and the number of time steps is 15000. The elapsed calculation time is 23178 s using the Star-CCM+ in-built function and 28233 s using the user code, which means 22 % increase in the calculation time.

3.3 Cnoidal waves

When the REEF3D simulation is coupled to the CFD simulation, (simulation nr. 4 and nr. 5) each time step from the REEF3D simulation is used directly in the interpolation files with the original REEF3D grid. REEF3D uses adaptive time steps which is limited by a given Courant number, in this simulation set to 0.1. The applied grid is uniform as shown in Figure 11 and the number of grid cells per wave length is set to 760 in the REEF3D simulations. These two simulations, coupled with REEF3D are carried out with two different forcing coefficients in

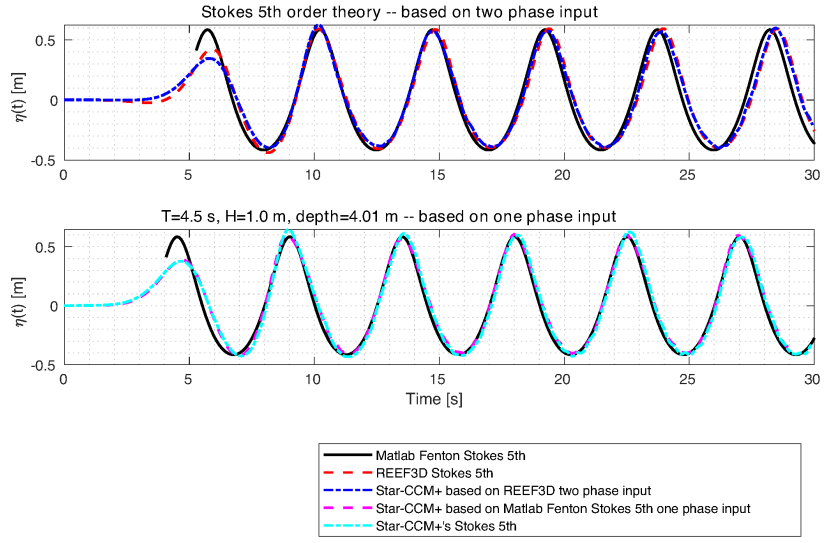

Figure 8: Comparison of the free surface elevation in the middle of the simulation zone

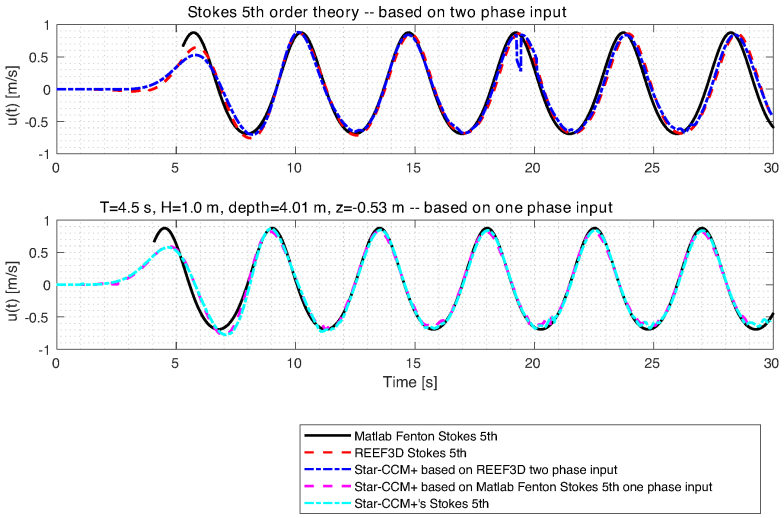

Figure 9: Comparison of the horizontal velocity components in the middle of the simulation zone at $z = -0.53$ m

the CFD simulations.

The accuracy of the interpolation grid is tested before the one-phase coupled simulation is started (simulation nr. 6). The number of cells per wave length is 440 and 60 cells per wave height. The same trend is observed regarding the vertical grid resolution and the maximum interpolation error as in the convergence study for the Stokes wave. For example, the change of resolution from 60 to 30 almost doubles the interpolation error of the horizontal velocity component from $2.25 \cdot 10^{-3}$ to $4.25 \cdot 10^{-4}$ (not shown in this paper).

The volume fraction of water is shown at the early stage of the simulation in Figure 12. The figure shows the whole domain and two close zooms of the free surface with the applied

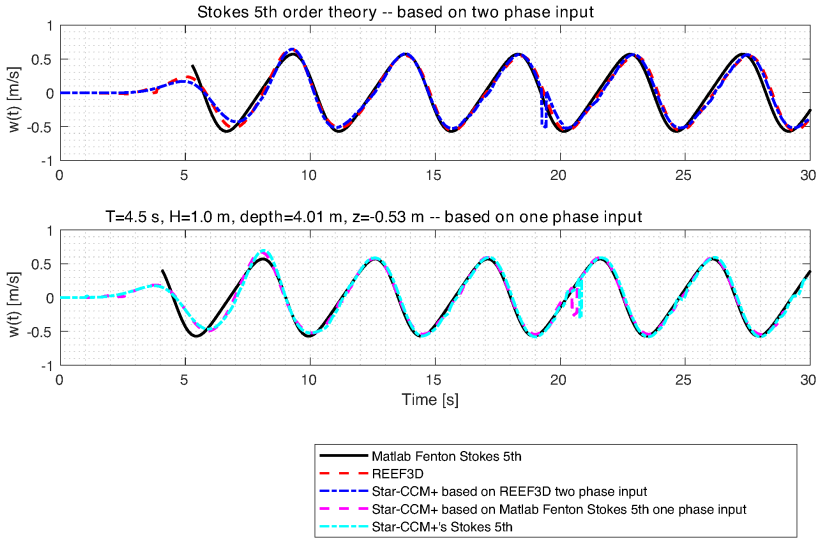

Figure 10: Comparison of the vertical velocity components in the middle of the simulation zone at $z = -0.53$ m

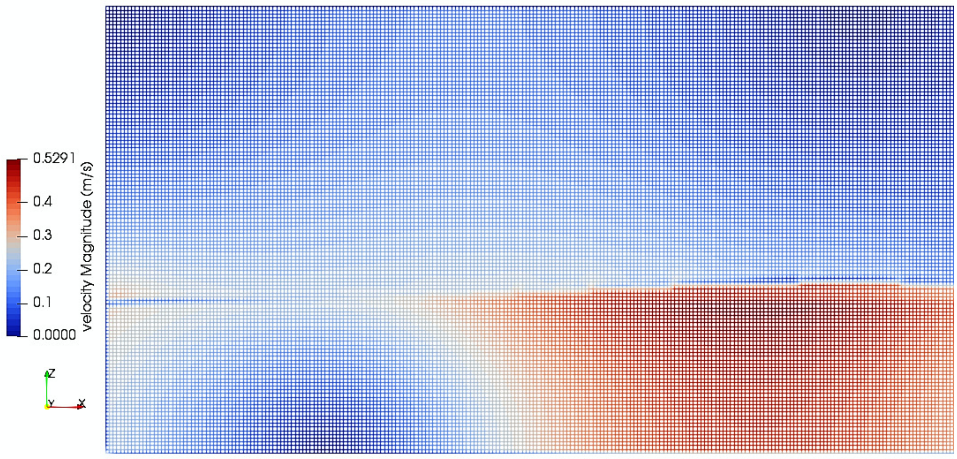

Figure 11: Mesh used in the REEF3D simulation and as interpolation grid

mesh. The interface between water and air in the wave generation zone (upper left picture) and in the simulation zone (upper right picture) is smooth. As in the previous simulation it is about 2 cells thick in the wave generation zone and one cell thick in the simulation zone. The magnitude of the velocity field, presented in Figure 13 shows good agreement between the REEF3D simulation and the coupled CFD simulation.

The three simulations as well as the the analytical solution generated with an in-house script are compared. The analytical solution is based on Cnoidal 2^{nd} order wave theory Sobey (1997) and is shown in Figure 14, 15 and 16 as black lines. The upper diagrams of Figure 14, 15 and 16 compares the original REEF3D simulations, based on Cnoidal 5^{th} order theory (red line) with the coupled CFD simulations (blue and cyan lines). The time series are synchronized with each other at the first zero-up-crossing of the free surface time series at $t = 12$ s. The REEF3D time series compare very well with the CFD simulations, except in the initial transient time regime. Here, one can observe the effect of the larger forcing coefficient

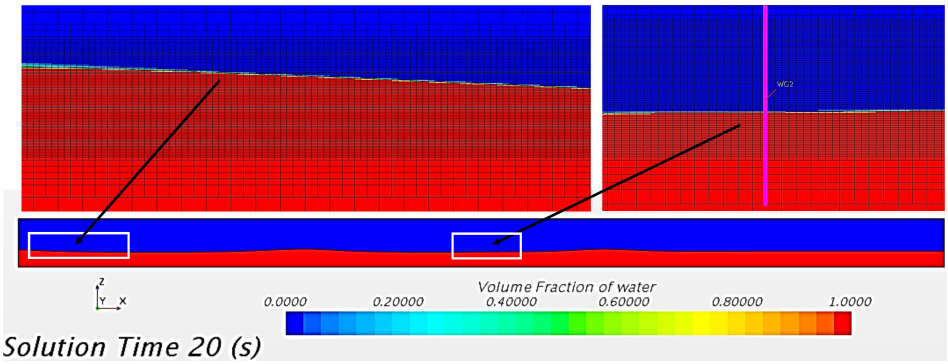

Figure 12: Volume of fraction of water in the Star-CCM+ simulation based coupled with the REEF3D simulation

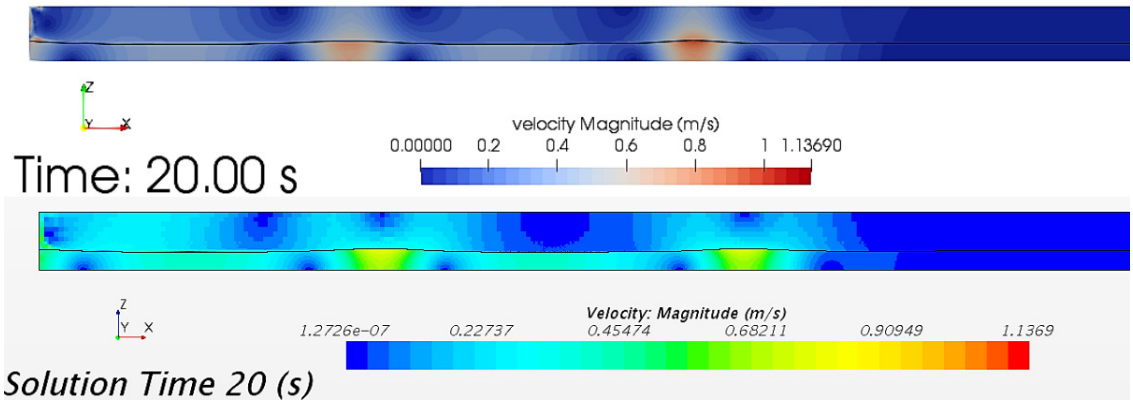

Figure 13: Comparison of the magnitude of the velocity between REEF3D simulation and Star-CCM+

which gives a better similarity between the coupled simulations red line and cyan line up to $t = 12$ s. After this time it is difficult to discover any differences between the three colored curves.

In the lower diagram of Figure 14, 15 and 16 the analytical solution based on the second order Cnoidal theory shows very good agreement with the CFD simulation. In this simulation the waves are generated with the interpolation files which are defined by this theory. One can conclude that the user code `table2D` function manages to generate very similar waves in the coupled CFD simulations.

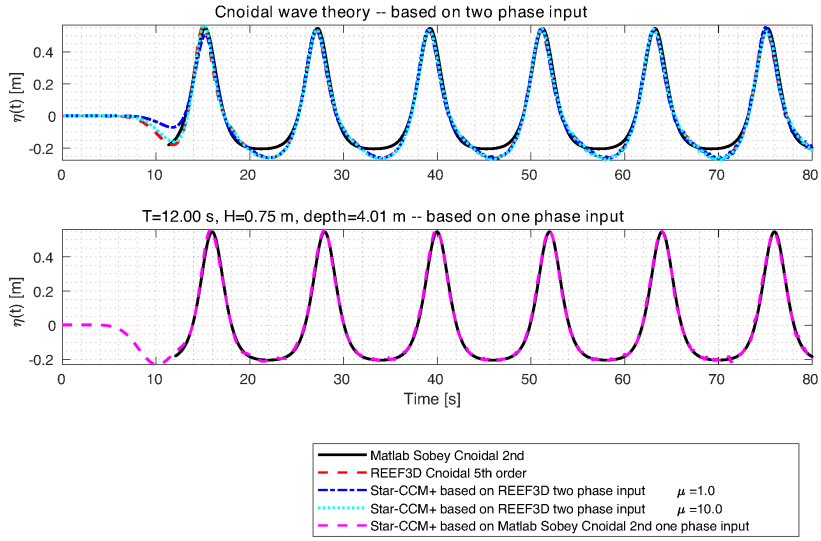

Figure 14: Comparison of the free surface elevation in the middle of the simulation zone

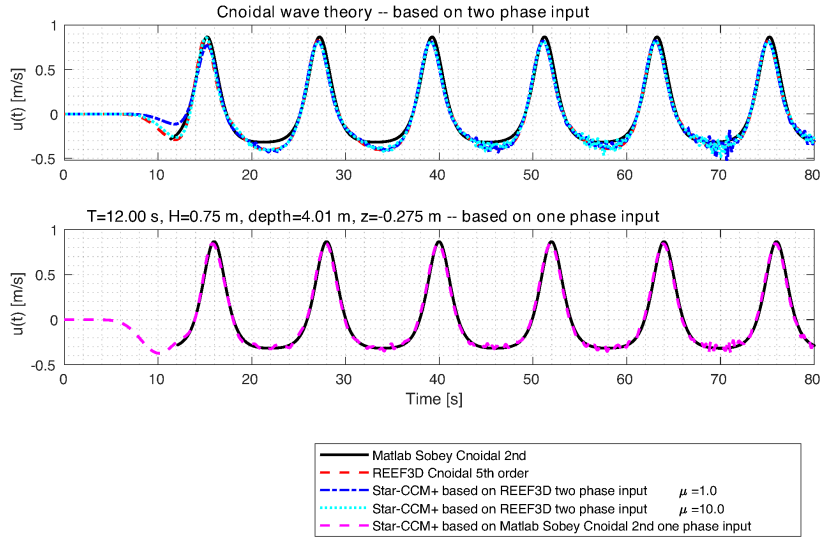

Figure 15: Comparison of the horizontal velocity components in the middle of the simulation zone at $z = -0.275$ m

3.4 Focused waves

For the verification we used the results from the simulation presented in Bihs et al. (2017). A focused wave group is simulated with REEF3D in a very short domain using linear wave theory to define the inlet boundary conditions. The wave packets generation uses a shape amplitude spectrum of the form Henning (2005):

$$A_i' = \frac{24\left(\omega_i - \omega_{beg}\right)\left(\omega_i - \omega_{end}\right)^2}{4\left(\omega_{end} - \omega_{beg}\right)^3} \tag{11}$$

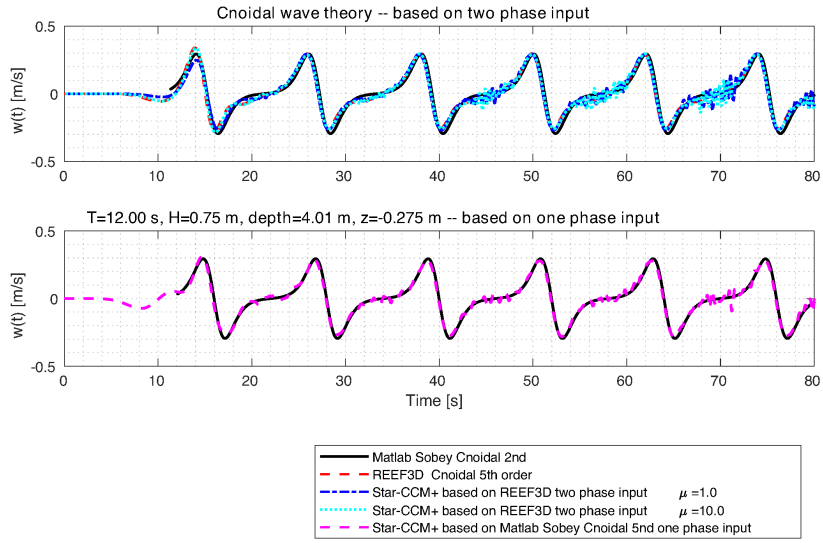

Figure 16: Comparison of the vertical velocity components in the middle of the simulation zone at $z = -0.275$ m

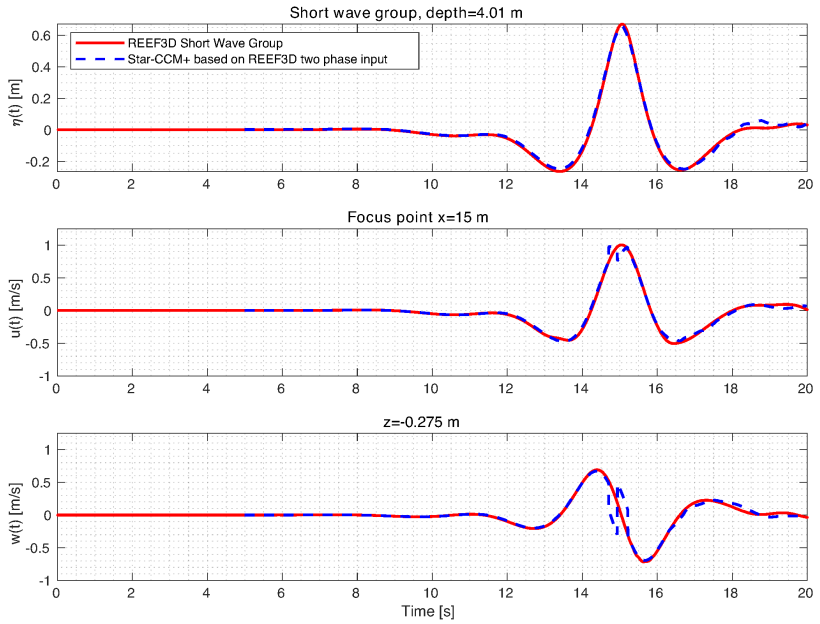

Figure 17: Comparison of the free surface elevation at the focus point $x = 15$ m

Here, ω_i is the angular frequency and the subscripts *beg* and *end* confine the Fourier spectrum on the frequency axis. The magnitude of the resulting wave amplitude A_i' does not represent the given focused wave input at this point, so a scaling factor f is calculated from the

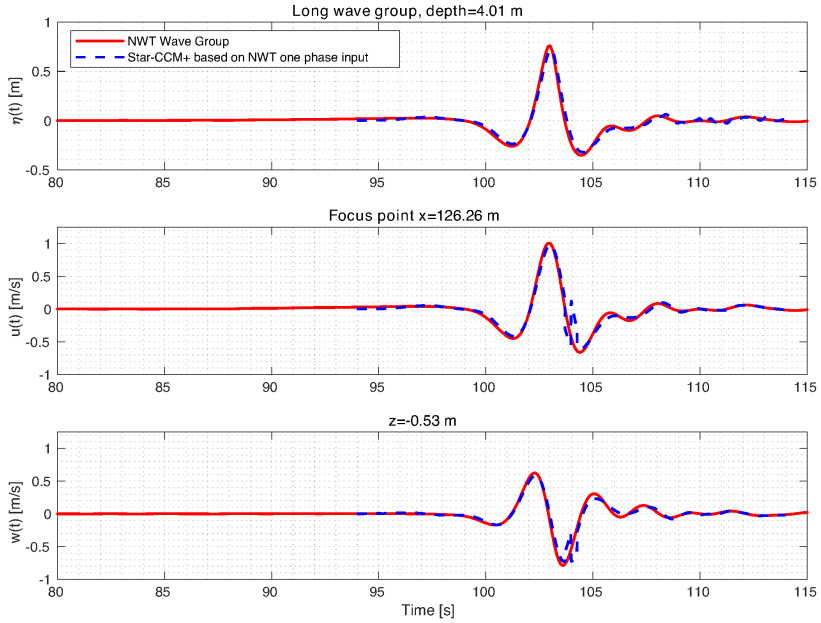

Figure 18: Comparison of the free surface elevation at the focus point

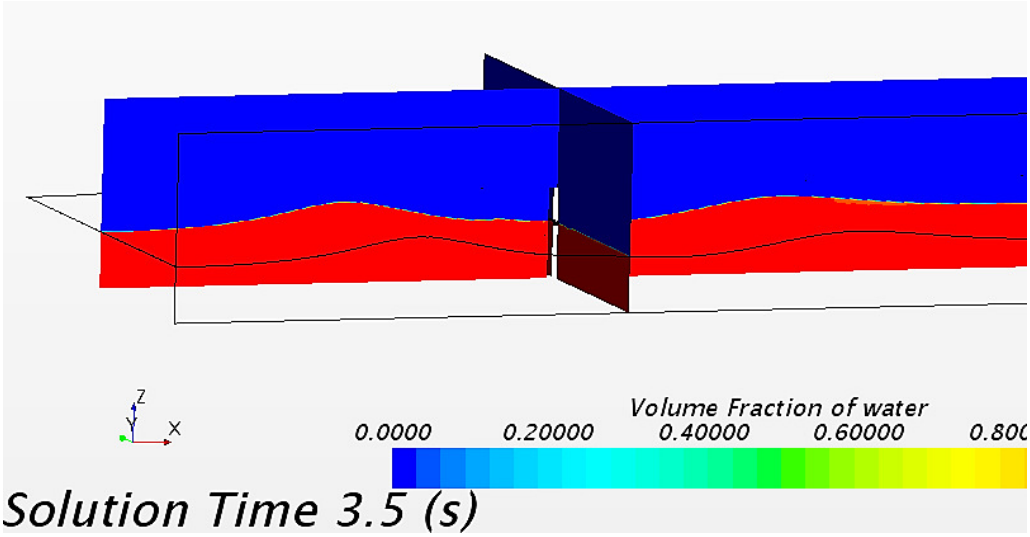

Figure 19: Star-CCM+ simulation setup with the volume of fraction of water

superposition of all waves with zero phase θ_i and with the given focusing amplitude A_{focus}:

$$A'_{focus} = \sum_{i=1}^{N} A'_i \cos(\theta_i) \quad f = \frac{A_{focus}}{A'_{focus}} \tag{12}$$

where N is the number of the wave elements. The typical number of the wave elements is between 50 and 100.

The wave group is focused over 15.00 m with a focusing amplitude $A_{focus} = 0.75$m and the spectrum has not zero value between 0.25 and 3.25 rad/s. The first 6 m of the REEF3D domain is used as interpolation data set for the coupled simulation. Every time step is used to generate the interpolation files, for every 0.01 s one interpolation file is defined. The comparison of the free surface elevation and the velocity components in Figure 17 shows very good agreement.

The results of a coupling with PNWT is presented in Figure 18. Here the same wave packet as the previous simulation is focused over 126.21 m in the PNWT. The free surface elevation and the velocity field of a small area between $x = 111.00$ m and $x = 117.00$ m are used to define the data set, which was used in the wave generation zone of the CFD simulation. The comparison of the calculated time series between the PNWT simulation and the CFD simulation shows very good agreement except at the the maximum crest height where the estimated free surface elevation as well as the velocity components are slightly lower in the CFD simulation. The reason for this difference may be explained by the large time steps of the interpolation tables, $dt = 0.1$ s relatively to the REEF3D coupled simulation.

3.5 Stokes wave with mono-pile

The last verification case where the 2D REEF3D simulation is coupled to a 3D CFD simulation with a mono-pile. This case was presented with the results of the 3D REEF3D simulation with the mono-pile and with the Star-CCM+ in-built function generated waves in Pakozdi

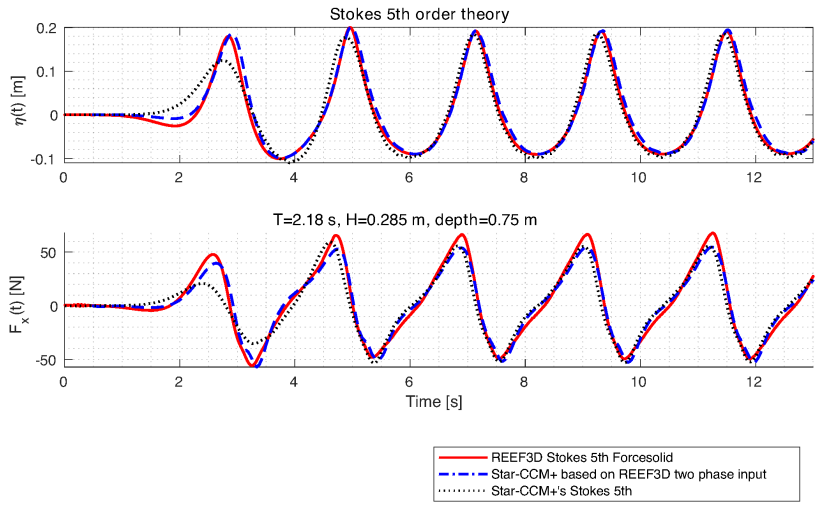

Figure 20: Comparison of the estimated global horizontal forces acting on the mono-pile

et al. (2018). The CFD setup is shown in Figure 19. The comparison of the free surface elevation without the mono-pile, (simulation nr. 9) is shown in the upper diagram of Figure 20. The red line presents the REEF3D results, the blue line presents this simulation coupled with CFD simulation results and the black line shows the Star-CCM+ simulation with its in-built function. One can observe a small divergence between the REEF3D simulated wave and the Star-CCM+ in-built wave model as previously observed for the deep water wave simulations. The difference between the estimated global horizontal force acting on the mono-pile calculated in REEF3D and in Star-CCM+ in-built wave model is larger in the lower diagram.

No significant difference in the calculation time between the coupled 3D CFD simulation and the uncoupled 3D CFD simulation was observed. Generally speaking the cost of the file operation and the interpolation is the 20 % increase in the elapsed calculation time between two 2D Star-CCM+ simulations with a small mesh (70 000 cells) while it is insignificant for the larger 3D simulation with a cell number larger than 3 million cells.

4 Conclusions

A file based one way coupling method between two numerical wave tank simulations is presented in this paper. The applied techniques are described in detail in the implementation section. Based on the presented results from the verification cases it can be concluded that this method is able to generate very similar waves in the coupled CFD simulation despite the relatively low order of the interpolation.

Acknowledgements

The authors are grateful to the grants provided by the Research Council of Norway under the INDNOR project (No. 246810) and WAS-XL project (No. 268182).

References

Aggarwal, A., Alagan Chella, M., Bihs, H., Pakzodi, C., Berthelsen, P.A. and Arntsen, Ø.A. (2017). Numerical investigation of irregular breaking waves for extreme wave spectra using CFD. In: *27th Annual International Ocean and Polar Engineering Conference*, ISOPE-I-17-460. San Francisco, California, USA.

Aggarwal, A., Pakozdi, C., Bihs, H., Myrhaug, D. and Alagan Chella, M. (2018). Free surface reconstruction for phase accurate irregular wave generation. *Journal of Marine Science and Engineering*, **6**(3). ISSN 2077-1312. 10.1115/1.404892510.3390/jmse6030105.

Alagan Chella, M., Bihs, H., Myrhaug, D. and Muskulus, M. (2015). Breaking characteristics and geometric properties of spilling breakers over slopes. *Coastal Engineering*, **95**, 4 – 19. ISSN 0378-3839. 10.1115/1.4048925https://doi.org/10.1016/j.coastaleng.2014.09.003.

Baquet, A., Kim, J. and Huang, Z. (2017). Numerical modeling using cfd and potential wave theory for three-hour nonlinear irregular wave simulations. In: *ASME 2017 36th OMAE*, OMAE2017-61090. Trondheim, Norway.

Bihs, H., Kamath, A., Chella, M.A., Aggarwal, A. and Arntsen, Ø.A. (2016). A new level set numerical wave tank with improved density interpolation for complex wave hydrodynamics. *Computers & Fluids*, **140**, 191 – 208. ISSN 0045-7930. 10.1115/1.4048925https://doi.org/10.1016/j.compfluid.2016.09.012.

Bihs, H., Kamath, A., Chella, M.A. and Arntsen, Ø.A. (2017). Extreme wave generation, breaking and impact simulations with REEF3D. In: *ASME 2017 36th OMAE*, OMAE2017-61524. Trondheim, Norway.

Bøckmann, A., Pákozdi, C., Kristiansen, T., Jang, H. and Kim, J. (2014). An experimental and computational development of a benchmark solution for the validation of numerical wave tanks. In: *ASME 2014 33rd OMAE*, OMAE2014-24658. San Francisco, California, USA. OMAE2014-24710.

Choi, Y., Bouscasse, B., Seng, S., Ducrozet, G., Gentaz, L. and Ferrant, P. (2018). Generation of regular and irregular waves in Navier-Stokes CFD solvers by matching with the nonlinear potential wave solution at the boundaries. In: *ASME 2018 37th OMAE*, OMAE2018-78077. Madrid, Spain.

Clauss, G.F., Stempinski, F., Stück, R. and Schmittner, C.E. (2006). Computational and experimental simulation of nonbreaking and breaking waves for the investigation of structural loads and motions. In: *ASME 2006 25th OMAE*, OMAE2006-92238. Hamburg, Germany.

Duz, B., Bunnik, T., Kapsenberg, G. and Vaz, G. (2016). Numerical simulation of nonlinear free surface water waves - coupling of a potential flow solver to a urans/vof code. In: *ASME 2016 35th OMAE*, OMAE2016-54808. Busan, South Korea.

Fenton, J. (1985). A fifth-order Stokes theory for steady waves. *Waterway Port Coastal and Ocean Engineering*, (111), 216–234.

Henning, J. (2005). *Generation and analysis of harsh wave environments*. Ph.D. thesis, TU Berlin.

Jacobsen, N. (2017). *waves2Foam Manual*.

Jacobsen, N.G., Fuhrman, D.R. and Fredsøe, Jørgen (2012). A wave generation toolbox for the open-source cfd library: Openfoam. *International Journal for Numerical Methods in Fluids*, **70**(9), 1073–1088. 10.1115/1.404892510.1002/fld.2726.

Kamath, A., Alagan Chella, M., Bihs, H. and Arntsen, Ø.A. (2015). Evaluating wave forces on groups of three and nine cylinders using a 3d numerical wave tank. *Engineering Applications of Computational Fluid Mechanics*, **9**(1), 343–354. 10.1115/1.404892510.1080/19942060.2015.1031318.

Kim, J., Jang, H., Izarra, R., Martin, D. and Dalane, O. (2014). CFD-FE simulation of wave slamming on an offshore platform in extreme sea states. In: *OTC 2014*. OTC-25423.

Kim, J., O'Sullivan, J. and Read, A. (2012). Ringing analysis of a vertical cylinder by Euler overlay method. In: *31st OMAE*. OMAE2012-84091.

Miquel, A.M., Kamath, A., Alagan Chella, M., Archetti, R. and Bihs, H. (2018). Analysis of different methods for wave generation and absorption in a CFD-based numerical wave tank. *Journal of Marine Science and Engineering*, **6**(2). ISSN 2077-1312. 10.1115/1.404892510.3390/jmse6020073.

Muzaferija, S. and Peric, M. (1999). Computation of free surface flows using interface-tracking and interface capturing methods. In: *Nonlinear Water Wave Interaction*, 59–100. WIT Press.

Ostman, A., C.Pakozdi, Sileo, L., Stansberg, C. and Silva, D.F.C. (2014). A fully nonlinear RANS-VOF numerical wavetank applied in the analysis of green water on fpso in waves. In: *Proceedings of the 33rd International Conference on Ocean, Offshore and Artic Engineering*, OMAE2014-23927. San Francisco, California, USA.

Pakozdi, C., Östman, A., Stansberg, C., Peric, M., Lu, H. and Baarholm, R. (2015). Estimation of wave in deck load using CFD validated against model test data. In: *25th Annual International Ocean and Polar Engineering Conference*, 2015-TPC-1134. Kona, Hawaii.

Pakozdi, C., Spence, S., Fouques, S., Thys, M., Alsos, H.S., Bachynski, E.E., Bihs, H. and Kamath, A. (2018). Nonlinear wave load models for extra large monopiles. In: *Proceedings of ASME 2018 1st International Offshore Wind Technical Conference*, IOWTC2018-1083. San Francisco, CA.

Peric, M. (2017). Prediction of wave propagation and wave-structure interaction. Power Point Presentation. Siemens AG.

Press, W., Teukolsky, S., Vetterling, W. and Flannery, B. (2007). *Numerical Recipes 3rd Edition: The Art of Scientific Computing*. Cambridge University Press. ISBN 9780521880688.

Simcenter (????). *Star-CCM+ 13.04 User Manual*. Simens PLM Software.

Sobey, R. (1997). Linear and nonlinear wave theory. Short advanced course, Leichtweiß-Institut für Wasserbau, Braunschweig.